Title

Renal Subcapsular xenografing of human fetal external genital tissue – A new model for investigating urethral development

Authors

Isaacson, Dylan
Shen, Joel
Cao, Mei
et al.

Publication Date

2017-11-01

DOI

10.1016/j.diff.2017.09.002

Peer reviewed

HHS Public Access

Author manuscript

Differentiation. Author manuscript; available in PMC 2018 November 01.

Published in final edited form as:

Differentiation. 2017 ; 98: 1–13. doi:10.1016/j.diff.2017.09.002.

Renal Subcapsular Xenografing of Human Fetal External Genital Tissue – A New Model for Investigating Urethral Development

Dylan Isaacson[1], **Joel Shen**[2], **Mei Cao**[2], **Adriane Sinclair**[2], **Xuan Yue**[2], **Gerald Cunha**[2], and **Laurence Baskin**[2,3,*]

[1]School of Medicine, University of California, San Francisco, San Francisco, CA

[2]Department of Urology, University of California, San Francisco, San Francisco, CA

[3]Division of Pediatric Urology, University of California San Francisco Benioff Children's Hospital, San Francisco, California

Abstract

In this paper, we introduce our novel renal subcapsular xenograft model for the study of human penile urethral and clitoral development. We grafted fifteen intact fetal penes and clitorides 8 to 11 weeks fetal age under the renal capsules of gonadectomized athymic mice. The mice were treated with a subcutaneous pellet of dihydrotestosterone (DHT), diethylstilbestrol (DES) or untreated with hormones. Xenografts were harvested after fourteen days of growth and analyzed via serial histologic sectioning and immunostaining for Ki-67, cytokeratins 6, 7 and 10, uroplakin and the androgen receptor. Non-grafted specimens of similar fetal age were sectioned and immunostained for the same antigenic markers. 14/15 (93.3%) grafts were successfully propagated and harvested. The developing urethral plate, urethral groove, tubular urethra, corporal bodies and preputial lamina were easily identifiable. These structures demonstrated robust cellularity, appropriate architecture and abundant Ki-67 expression. Expression patterns of cytokeratins 6, 7 and 10, uroplakin and the androgen receptor in xenografted specimens demonstrated characteristic male/female differences analogous to non-grafted specimens. DHT treatment reliably produced tubularization of nascent urethral and vestibular structures and male patterns of androgen receptor expression in grafts of both genetic sexes while estrogenic or hormonally absent conditions reliably resulted in a persistent open urethral/vestibular groove and female patterns of androgen receptor expression. This model's success enables further study into causal pathways by which endocrine-disrupting and endocrine-mimicking substances may directly cause disruption of normal human urethral development or hypospadias.

Keywords

Hypospadias; urethra; genital tubercle; xenograft; endocrine disruptors; nude mouse

[*]Address Correspondence to: Laurence Baskin, Laurence.Baskin@ucsf.edu, 513 Parnassus Ave, Health Sciences West, Room 1434, San Francisco, CA, 94143.

Introduction

Hypospadias is the second-most-common congenital anomaly of the urogenital tract, occurring in 1:200 to 1:300 live male births in the USA [1–3]. Hypospadias is an abnormality of urethral development characterized by an ectopic urethral meatus on the ventral aspect of the penis, an abnormal urethral corpus spongiosum, penile curvature and foreskin abnormalities [4, 5]. Office visits, surgical treatment and hospital recovery together constitute a substantial cost to the healthcare system [6]. Patients with hypospadias seek sexual contacts and engage in sexual intercourse at lower rates than age-matched controls and are significantly more likely to report dissatisfaction with their genitals [5]. While the etiology of hypospadias remains unknown, both genetic susceptibility and environmental exposures appear to contribute [7–11]. Environmental exposures to estrogens, anti-androgens, and industrial and agricultural chemicals cause hypospadias in laboratory animals and have been linked to hypospadias in human epidemiologic studies [12–14]. Human males exposed in utero to the xenoestrogen diethylstilbestrol (DES) have an increased incidence of hypospadias [15–17]. A recent multicenter study showed a strong association between parental occupational and environmental exposures to endocrine disruptors such as solvents, adhesives, Bisphenol A (BPA), pesticides, phthalates and flame retardants and development of hypospadias in male children (OR 3.13 95% CI 2.11–4.65) [18].

The two most widely used models for the study of hypospadias in the laboratory are the mouse and rat [19–22]. Extensive efforts have focused on understanding urethral development in these species [23–28]. Unfortunately, rats and mice are imperfect models of human hypospadias for multiple reasons, including the presence of penile cartilage and bone [22, 24], the existence of internal and external prepuces, low rates of spontaneous (non-induced) hypospadias and the absence of perineal or penile-shaft hypospadias [19, 20]. As morphogenic mechanisms of penile urethral development in rodents are radically different from human mechanisms (Fig. 1), it is not surprising that murine “hypospadias” is substantially different morphologically from the condition seen in humans [19]. Given these vast anatomic differences, it has become apparent that to fully understand human hypospadias, the focus must be on human urethral development. Definitive proof that environmental agents adversely affect human penile urethral development should come from direct testing of endocrine agents on human fetal organs.

There is an extensive literature on xenogransplantation of human fetal tissue into immunodeficient mice stretching back to 1974, when Povlsen et al. demonstrated successful propagation and histologic preservation of human fetal thymic, lung, pancreatic, adrenal, renal, testicular and ovarian tissue grown subcutaneously in athymic mice for 5–64 days [29]. Since this time, researchers have demonstrated normal growth and normal differentiation of human fetal intestine [30], skin [31], lung [32], male and female reproductive tract [33–35], prostate [36, 37] and ovary [38] transplanted into athymic or severe combined immunodeficient (SCID) mice. Graft differentiation with measurable production of circulating graft-specific hormones has been demonstrated in xenografted human fetal pancreas [39–41], pituitary [42] and testis [43].

Xenotransplantation provides a powerful model to ethically evaluate the effects of therapeutics and toxicants on target human tissues. Grafted cancer cells from a wide range of primary sites demonstrate high engraftment rates, biological stability and preservation of tumor architecture and molecular markers in immunodeficient mice, allowing for evaluation and development of novel anticancer agents [44, 45]. Intact xenografted human fetal internal reproductive organs have been extensively used to study the teratogenic effects of progesterone, diethylstilbestrol and other xenoestrogens on the developing prostate [36, 37] and female genital tract [34, 35, 46]. Grafted organs in these models demonstrate high engraftment rates in both control and toxicant groups under a variety of experimental conditions.

Human tissue xenografts have been successfully propagated utilizing a variety of locations within the immunocompromised mouse, including subcutaneous [29, 30, 40], renal subcapsular [33, 37, 46, 47], orthotopic [48–50] and intraperitoneal [49, 51, 52] sites. While orthotopic and intraperitoneal sites have advantages in promoting tumor growth and metastasis in experiments with human cancer cells, the subcutaneous and renal subcapsular sites have been more extensively utilized in xenotransplantation of intact human fetal organs. The subcutaneous site has the advantages of easy access and large surface area and provides the ability to visually and non-invasively monitor the growth of the graft, however graft take rates are low. The renal subcapsular site is more extensively vascularized, resulting in graft take rates approaching 100% [45, 47].

In the absence of a suitable animal model to study human urethral development, hypospadias and the effects of exogenous hormones, endocrine disruptors and toxicants on these processes, we have developed a novel and ethical system of investigation. In this work, we describe our renal subcapsular xenografting model for the study of urethral development utilizing human fetal penes and clitorides grown in athymic mouse hosts. We demonstrate a high rate of engraftment, normal patterns of morphologic development, normal differential gene expression and feasibility of growth in varying hormonal environments.

Methods

Human fetal external genital specimens were collected following elective pregnancy termination procedures with approval by the institutional review board at the University of California, San Francisco (UCSF). Collected specimens were placed in phosphate-buffered saline (PBS) on ice for transport from procedure rooms. Male and female genital tubercles were isolated under a dissecting microscope (Zeiss Stemi 2000-C, Carl Zeiss Ag, Oberkochen, Germany) and stored at 2°C in RPMI 1640 medium (UCSF Cell Culture Facility, San Francisco, CA, USA) for no more than 24 hours before grafting. Specimen age was estimated using heel-toe length [53]. Sex was determined by polymerase chain reaction (PCR) of the sex-determining region Y (SRY) gene, morphology of Wolffian and Mullerian structures and/or presence of testes or ovaries [54].

All grafting procedures were performed in our IACUC-approved facility at UCSF. Immediately prior to grafting, genital tubercles were transected at the most proximal point

on the penile/clitoral shaft to excise any pre-existing tubular urethra from the specimen (Fig. 2).

In this way, urethral formation during the growth period could be attributed to developmental events post-grafting. Specimens were transplanted under the renal capsule of athymic nude mice (CD-1 NU/NU, Charles River Laboratories, Wilmington, MA) as previously described [47] and a suture was placed to demarcate the distal end of the graft. To achieve a standardized hormonal milieu for xenograft growth, mouse hosts were castrated to eliminate endogenous sex steroids. Following gonadectomy, mouse adrenal glands do not compensate by producing bioactive levels of estrogens or androgens [55]. We confirmed the absence of trophic sex hormones of adrenal origin in castrated hosts by monitoring the atrophic status of the host's prostate via wet weight and histology. In a subset of our grafts, a 25mg pellet of dihydrotestosterone (DHT) (A8380, Sigma-Aldrich, St. Louis, MO, USA) or diethylstilbestrol (DES) (D4628, Sigma-Aldrich, St. Louis, MO, USA) was implanted subcutaneously at the time of grafting and gonadectomy. Our selection of DHT instead of testosterone eliminates the possibility of aromatase-mediated conversion of testosterone to estradiol. Grafts were grown for 14 days, at which time the animals were euthanized and the grafts harvested. Grafts were fixed in 10% neutral buffered formalin for 48 hours, embedded in paraffin, serially sectioned at 5 microns on a microtome (Leica RM2135, Leica Microsystems, Wetzlar, Germany) and applied to glass slides (Fisherbrank Superfrost Plus, Thermo Fisher Scientific, Waltham MA, USA). Non-grafted external genital specimens of similar fetal age were fixed and prepared in identical fashion for comparison with xenografts.

Every 20th section was stained with hematoxylin and eosin (H&E) to highlight tissue architecture. Intervening slides were immunoassayed with primary antibodies against cytokeratins 6 (K6), 7 (K7) and 10 (K10), uroplakin, Ki-67 and the androgen receptor (AR). Slides were counterstained with Hoechst (33258) dye to highlight tissue architecture and to distinguish xenograft tissue of human origin from the cells of the host mouse kidney [56]. Primary and secondary antibodies used and their dilutions are detailed in Table 1. Regarding antigenic targets of immunostaining, cytokeratins are intermediate filament proteins that provide mechanical support to epithelia [57, 58]. K6 is present in the basal and intermediate layers of urothelium and epidermis as well as the urethral plate of developing external genitalia. K7 is found in the apical layer of urothelium only. K10 is present in epidermis but is absent in normal urothelium. Uroplakin is a highly-specific urothelial marker absent in other tissue types [59]. Ki-67 is a specific marker for actively proliferating cells [60]. The androgen receptor is a nuclear receptor activated by androgenic hormone binding whose activity as a transcription factor appears to be critical in early development of male internal and external genitalia [61].

Stained slides were visualized on a light microscope (Leica DM4000B, Leica Microsystems, Wetzlar, Germany) and photographed using Leica Application Suite V 4.1.0 (Leica Microsystems, Wetzlar, Germany). Digital images were enlarged and overlaid using Adobe Photoshop (Adobe Systems, San Jose, CA, USA). Brightness and color balance were adjusted in Adobe Photoshop, however no specific features were enhanced, obscured or moved.

Results

Fifteen fetal male and female external genital specimens aged 8–11 weeks at the time of collection were grafted. Fourteen grafts (93.3%) were successfully harvested. In all of these specimens, developing urethral and vestibular structures were well-preserved. Focal areas of central necrosis were observed in 5/14 (35.7%) specimens, however in none of these grafts did necrosis include the developing urethra or vestibule. Graft health correlated with robust expression of Ki-67 in the grafts (Fig. 3). In all grafts evaluated, Ki-67 expression was increased in the area of the urethral plate and urethral groove.

Male Graft Results

Figure 4 depicts a non-grafted 11-week penis stained for K6, K7 and K10 demonstrating normal architecture. K6 staining highlights the urethral plate with K7 absent in this region (Fig. 4A). At mid-shaft, K6 is expressed in basal epithelial cells of the open urethral groove with K7 staining apical epithelial cells in the dorsal aspect of the urethral groove only (Fig. 4B). K6/K7 in proximal sections fully circumscribes the tubularized urethra (Fig. 4C) with K6 in basal epithelial cells and K7 in apical epithelial cells. In all grafted specimens, uroplakin was expressed in apical epithelial cells in the same areas as K7 (Fig. 5).

Figure 6 shows a graft of an 8-week penis grown in the presence of DHT. This graft has formed a tubular urethra. Some distortion of architecture is observed due to the compressive effects of the renal capsule. However, regions of K6, K7, K10 and uroplakin staining analogous to those in the non-grafted 11-week penis (Fig. 4) are identifiable. In this graft, K6 is present in basal cells of the surface epidermis, urethral plate and basal layers of the urethral groove and nascent tubularized urethra. K7 and uroplakin (not illustrated) are absent in the surface epithelium and urethral plate, but co-expressed in the apical layers of the urethral groove (Fig. 6B) and in the tubularized urethra (Fig. 6C). K10 is present in epidermal layers but absent in urethral structures.

Conversely, in grafted male specimens grown in the presence of DES (not shown) or in the absence of hormones, tubular urethral structures are not observed at any point in the graft. In the depicted 9-week penile graft grown without hormones (Fig. 7), K6 stains the urethral plate with K7 apical to K6 in the dorsal aspect of the urethral groove. Likewise, K10 is only present in epidermal structures as is witnessed in non-grafted female specimens (Fig. 8) and female grafts grown in the absence of androgen (Fig. 9).

Female Graft Results

Figure 8 depicts a non-grafted 11-week clitoris stained for K6, K7 and K10. K6 is present in the distal vestibular plate with K7 absent (Fig. 8A). At mid-shaft, K6 is present in basal epithelial cells of the vestibular groove with K7 present in apical cells of the dorsum of the groove only (Fig. 8B). K10 is present in apical cell layers only in ventral and lateral aspects of the vestibular groove and in the epidermis (Fig. 8E). Proximally, K6 demarcates basal epithelial cells of the entire clitoral vestibule with K7 present apically only in the dorsal region (Fig. 8C) and K10 present only in apical cells of the ventral and lateral regions of the vestibule (Fig. 8F).

The clitoral graft grown in a castrated host without endogenous sex hormones (Fig. 9) has formed an open vestibular groove. In this graft, K6 is present in the vestibular plate and in basal cells of the surface epidermis and the vestibular groove. The proximal vestibule is not easily identified due to distortion from the renal capsule. K7 and uroplakin (not illustrated) are absent in the surface epidermis and vestibular plate, but are seen in apical layers of the dorsal aspect of the vestibular groove (Fig. 9B, C). K10 is present in superficial epidermal layers. The presence of K10 in lateral/ventral regions of the vestibular groove and its absence in the dorsal aspects of the vestibular groove are characteristic of the normal vestibular groove.

Conversely, grafted female specimens grown in the presence of DHT (Figs. 10, 11) formed tubular urethras. The urethral structure in a 9.5-week clitoris grown for two weeks with DHT (Fig. 10C) is circumferentially demarcated by K7 and uroplakin with K10 absent as is seen in normal male specimens (Fig. 4) and male grafts grown in the presence of DHT (Fig. 6). The urethral structure shown in an 8.5-week clitoral specimen grown for two weeks with DHT (Fig. 11C) is undergoing fusion and is similarly circumscribed by K7 and uroplakin with K10 absent.

Androgen Receptor Results

Androgen receptor staining was prominently expressed in epithelial cells of the roof of the urethral groove and lateral urethral folds of both non-grafted male specimens (Fig. 12A) and male specimens grown in the presence of DHT (Fig. 12B). AR expression is reduced in penile specimens grown in the absence of androgen (Fig. 12C). AR is sparsely expressed in the epithelium of the roof of the vestibular groove and the vestibular folds of non-grafted clitoral specimens (Fig. 12D) and clitoral xenografts grown in the absence of androgen (Fig. 12E). Clitoral xenografts grown in the presence of DHT exhibit extensive AR staining in the roof and lateral aspects of the vestibular groove (Fig. 12F) as is observed in normal male specimens.

Discussion

This paper presents our renal subcapsular xenograft model for the study of the development of human external genitalia. To the extent of our knowledge, this is the first report of successful xenotransplantation and growth of intact human fetal penes and clitorides in immunocompromised animal hosts. Our graft take rate of 93% is consistent with the high success rates seen in other whole-organ renal subcapsular xenograft studies [33, 37, 46, 54] and provides further evidence of the value of this highly vascularized site in xenotransplantation experiments. Central necrosis was seen to variable degrees in 35% of the xenografts, a result that correlated with lower Ki-67 expression in these specific areas. This problem can be ameliorated by grafting younger, smaller specimens, by placing specimens in cold medium as soon as possible, and by grafting them as soon as possible. These steps have reduced this problem in the course of our experiments.

Recent studies by our group have elucidated mechanisms of human penile urethral and clitoral development [62, 63]. The urethra in the penile shaft forms via distal canalization of a solid urethral plate to form a wide-open urethral groove, followed by proximal to distal

fusion of the urethral folds, a process far more complicated than originally envisioned [64]. This results in formation of the tubular penile urethra and superficial midline penile raphe. In the clitoral shaft, distal canalization of the analogous solid vestibular plate is not followed by fusion of the vestibular folds, resulting in the open clitoral vestibule. Immunostaining of non-grafted specimens for cytokeratins 6, 7 and 10 consistently reveals characteristic male/female differences in expression. We have consistently observed patterns of cytokeratin staining analogous to non-grafted specimens in our penile xenografts grown in the presence of exogenous DHT and in clitoral xenografts grown in the absence of androgen. These morphologic results indicate that developmental processes in external genital xenografts proceed in a similar fashion to those seen *in vivo*.

Our observations of rich androgen receptor staining present in the urethral folds of normal male specimens and its relative absence in corresponding areas of normal female specimens contribute to of our hypothesis that fusion at the urethral groove to form the male tubularized penile urethra is mediated in part by androgen receptor-mediated signaling in the urethral folds. These processes occur in developing external genitalia between 8–12 weeks of fetal age and are demonstrated upon serial sectioning of specimens of these ages. Androgen receptor staining patterns in our xenografts are analogous to those seen in non-grafted specimens when male grafts are grown with DHT and female grafts grown in its absence. These expression patterns were reversed when male grafts are grown in the absence of androgen and female grafts in the presence of DHT. Our observation of androgen receptor upregulation in the lateral aspects of the vestibular grooves of female grafts grown with DHT align with our observations of tubularization in more proximal sections of those same grafts. These observations are consistent with the hypothesis that expression of the androgen receptor is itself androgen-regulated [61, 65]. Further experimentation in human genital xenografts at the genetic level should corroborate these observations by examining levels of AR-dependent nucleic acid transcription in these same areas.

We hypothesize that interruption of the canalization and/or fusion processes by exogenous substances with hormonal activity may contribute to the constellation of urethral and penile abnormalities seen in human hypospadias. Our xenografts have demonstrated robust growth under varied hormonal growth conditions. This has held true in non-physiologic scenarios. i.e. when male grafts were grown in DES-treated hosts or in the absence of androgen and when female grafts were grown in androgenic conditions. Our findings of interrupted urethral fusion in male grafts grown without androgen and induced urethral tubularization in female grafts grown in the presence of androgen are consistent with prior animal studies [65] and the human phenotypes seen in severe cases of congenital adrenal hyperplasia and in complete androgen insensitivity syndrome [66–68]. Our ability to selectively induce male and female phenotypes in this model will enable specific characterization and selective manipulation of androgen-dependent gene pathways as well as controlled experiments with endocrine-disrupting or endocrine-mimicking chemicals.

Our model has several potential limitations – we have not yet performed experiments defining optimal growth times or the ideal level to transversely excise the external genital from the anterior body wall to promote proximal fusion of the urethral groove. Further experiments are needed to evaluate the interactions between exogenous substances and

endogenous levels of hormones simulating situations occurring in our human environment. In presenting this model, we aim to enable these studies and further work establishing potential causal pathways of endocrine alteration, abnormal urethral development and human hypospadias.

Acknowledgments

Funding Sources

This work was supported by the National Institutes of Health [R01 DK058105/DK/NIDDK (LB), K12 DK083021/DK/NIDDK (AS)]; The American Urological Association/Urology Care Foundation Herbert Brendler, MD Research Fellowship (DI); The Alpha Omega Alpha Honor Medical Society Carolyn L. Kuckein Medical Student Research Fellowship (DI); and a Pathways to Discovery Project Grant from the University of California, San Francisco (DI)

References

1. Paulozzi L, Erickson D, Jackson R. Hypospadias Trends in Two US Surveillance Systems. Pediatrics. 1997; 100(5):831–834. [PubMed: 9346983]
2. Paulozzi LJ. International trends in rates of hypospadias and cryptorchidism. Environ Health Perspect. 1999; 107(4):297–302. [PubMed: 10090709]
3. Gallentine ML, Morey AF, Thompson IM Jr. Hypospadias: a contemporary epidemiologic assessment. Urology. 2001; 57(4):788–90. [PubMed: 11306407]
4. Baskin LS. Hypospadias and urethral development. J Urol. 2000; 163(3):951–6. [PubMed: 10688029]
5. Mieusset R, Soulie M. Hypospadias: psychosocial, sexual, and reproductive consequences in adult life. J Androl. 2005; 26(2):163–8. [PubMed: 15713818]
6. Pohl HG, et al. Cryptorchidism and hypospadias. J Urol. 2007; 177(5):1646–51. [PubMed: 17437777]
7. Kalfa N, et al. Hypospadias: interactions between environment and genetics. Mol Cell Endocrinol. 2011; 335(2):89–95. [PubMed: 21256920]
8. Yiee JH, Baskin LS. Environmental factors in genitourinary development. J Urol. 2010; 184(1):34–41. [PubMed: 20478588]
9. Hsieh MH, et al. Associations among hypospadias, cryptorchidism, anogenital distance, and endocrine disruption. Curr Urol Rep. 2008; 9(2):137–42. [PubMed: 18419998]
10. Choudhry S, et al. Genetic polymorphisms in ESR1 and ESR2 genes, and risk of hypospadias in a multiethnic study population. J Urol. 2015; 193(5):1625–31. [PubMed: 25463985]
11. van der Zanden LF, et al. Common variants in DGKK are strongly associated with risk of hypospadias. Nat Genet. 2011; 43(1):48–50. [PubMed: 21113153]
12. Kim KS, et al. Induction of hypospadias in a murine model by maternal exposure to synthetic estrogens. Environ Res. 2004; 94(3):267–75. [PubMed: 15016594]
13. Kojima Y, et al. Spermatogenesis, fertility and sexual behavior in a hypospadiac mouse model. J Urol. 2002; 167(3):1532–7. [PubMed: 11832783]
14. Gray LE Jr, Ostby JS, Kelce WR. Developmental effects of an environmental antiandrogen: the fungicide vinclozolin alters sex differentiation of the male rat. Toxicol Appl Pharmacol. 1994; 129(1):46–52. [PubMed: 7974495]
15. Henderson B, et al. Urogenital tract abnormalities in sons of women treated with diethylstilbestrol. Pediatrics. 1976; 58:505–507. [PubMed: 972792]
16. Klip H, et al. Hypospadias in sons of women exposed to diethylstilbestrol in utero: a cohort study. Lancet. 2002; 359(9312):1102–7. [PubMed: 11943257]
17. Bibbo M, et al. Follow-up study of male and female offspring of DES-exposed mothers. Obstet Gynecol. 1977; 49(1):1–8. [PubMed: 318736]

18. Kalfa N, et al. Is Hypospadias Associated with Prenatal Exposure to Endocrine Disruptors? A French Collaborative Controlled Study of a Cohort of 300 Consecutive Children Without Genetic Defect. Eur Urol. 2015
19. Cunha GR, et al. Current understanding of hypospadias: relevance of animal models. Nat Rev Urol. 2015; 12(5):271–80. [PubMed: 25850792]
20. Sinclair AW, et al. Mouse hypospadias: A critical examination and definition. Differentiation. 2016; 92(5):306–317. [PubMed: 27068029]
21. Sinclair AW, et al. Flutamide-induced hypospadias in rats: A critical assessment. Differentiation. 2016; 94:37–57. [PubMed: 28043016]
22. Phillips TR, et al. A Comprehensive Atlas of the Adult Mouse Penis. Sex Dev. 2015; 9(3):162–72. [PubMed: 26112156]
23. Rodriguez E Jr, et al. Specific morphogenetic events in mouse external genitalia sex differentiation are responsive/dependent upon androgens and/or estrogens. Differentiation. 2012; 84(3):269–79. [PubMed: 22925506]
24. Rodriguez E Jr, et al. New insights on the morphology of adult mouse penis. Biol Reprod. 2011; 85(6):1216–21. [PubMed: 21918128]
25. Weiss DA, et al. Morphology of the external genitalia of the adult male and female mice as an endpoint of sex differentiation. Mol Cell Endocrinol. 2012; 354(1–2):94–102. [PubMed: 21893161]
26. Mahawong P, et al. Comparative effects of neonatal diethylstilbestrol on external genitalia development in adult males of two mouse strains with differential estrogen sensitivity. Differentiation. 2014; 88(2–3):70–83. [PubMed: 25449353]
27. Mahawong P, et al. Prenatal diethylstilbestrol induces malformation of the external genitalia of male and female mice and persistent second-generation developmental abnormalities of the external genitalia in two mouse strains. Differentiation. 2014; 88(2–3):51–69. [PubMed: 25449352]
28. Blaschko SD, et al. Analysis of the effect of estrogen/androgen perturbation on penile development in transgenic and diethylstilbestrol-treated mice. Anat Rec (Hoboken). 2013; 296(7):1127–41. [PubMed: 23653160]
29. Povlsen CO, et al. Heterotransplantation of human foetal organs to the mouse mutant nude. Nature. 1974; 248(445):247–9. [PubMed: 4594645]
30. Winter HS, et al. Human intestine matures as nude mouse xenograft. Gastroenterology. 1991; 100(1):89–98. [PubMed: 1983853]
31. Lane AT, Scott GA, Day KH. Development of human fetal skin transplanted to the nude mouse. J Invest Dermatol. 1989; 93(6):787–91. [PubMed: 2584745]
32. Groscurth P, Tondury G. Cytodifferentiation of human fetal lung tissue following transplantation into "nude" mice. Anat Embryol (Berl). 1982; 165(2):291–302. [PubMed: 6760745]
33. Taguchi O, et al. Timing and irreversibility of Mullerian duct inhibition in the embryonic reproductive tract of the human male. Dev Biol. 1984; 106(2):394–8. [PubMed: 6548718]
34. Robboy SJ, Taguchi O, Cunha GR. Normal development of the human female reproductive tract and alterations resulting from experimental exposure to diethylstilbestrol. Hum Pathol. 1982; 13(3):190–8. [PubMed: 7076207]
35. Taguchi O, Cunha GR, Robboy SJ. Experimental study of the effect of diethylstilbestrol on the development of the human female reproductive tract. Biol Res Pregnancy Perinatol. 1983; 4(2):56–70. [PubMed: 6882849]
36. Sugimura Y, et al. Temporal and spatial factors in diethylstilbestrol-induced squamous metaplasia of the developing human prostate. Hum Pathol. 1988; 19(2):133–9. [PubMed: 3343029]
37. Yonemura CY, et al. Temporal and spatial factors in diethylstilbestrol-induced squamous metaplasia in the developing human prostate. II. Persistent changes after removal of diethylstilbestrol. Acta Anat (Basel). 1995; 153(1):1–11. [PubMed: 8560954]
38. Poulain M, et al. Involvement of doublesex and mab-3-related transcription factors in human female germ cell development demonstrated by xenograft and interference RNA strategies. Mol Hum Reprod. 2014; 20(10):960–71. [PubMed: 25082981]

39. Usadel KH, et al. Transplantation of human fetal pancreas: experience in thymusaplastic mice and rats and in a diabetic patient. Diabetes. 1980; 29(Suppl 1):74–9.
40. Tuch BE, et al. Histologic differentiation of human fetal pancreatic explants transplanted into nude mice. Diabetes. 1984; 33(12):1180–7. [PubMed: 6149970]
41. Peterson CM, et al. Human fetal pancreas transplants. J Diabet Complications. 1989; 3(1):27–34. [PubMed: 2523402]
42. Bastert G, et al. Heterotransplantation of human fetal pituitaries in nude mice. Endocrinology. 1977; 101(2):365–8. [PubMed: 885108]
43. Mitchell RT, et al. Xenografting of human fetal testis tissue: a new approach to study fetal testis development and germ cell differentiation. Hum Reprod. 2010; 25(10):2405–14. [PubMed: 20683063]
44. Jin K, et al. Patient-derived human tumour tissue xenografts in immunodeficient mice: a systematic review. Clin Transl Oncol. 2010; 12(7):473–80. [PubMed: 20615824]
45. Wang Y, et al. Development and characterization of efficient xenograft models for benign and malignant human prostate tissue. Prostate. 2005; 64(2):149–59. [PubMed: 15678503]
46. Cunha GR, et al. Absence of teratogenic effects of progesterone on the developing genital tract of the human female fetus. Hum Pathol. 1988; 19(7):777–83. [PubMed: 3402971]
47. Cunha GR, Baskin L. Use of sub-renal capsule transplantation in developmental biology. Differentiation. 2016; 91(4–5):4–9. [PubMed: 26639079]
48. Manzotti C, Audisio RA, Pratesi G. Importance of orthotopic implantation for human tumors as model systems: relevance to metastasis and invasion. Clin Exp Metastasis. 1993; 11(1):5–14. [PubMed: 8422706]
49. Shaw TJ, et al. Characterization of intraperitoneal, orthotopic, and metastatic xenograft models of human ovarian cancer. Mol Ther. 2004; 10(6):1032–42. [PubMed: 15564135]
50. Wang Y, et al. An orthotopic metastatic prostate cancer model in SCID mice via grafting of a transplantable human prostate tumor line. Lab Invest. 2005; 85(11):1392–404. [PubMed: 16155594]
51. Ward BG, et al. Intraperitoneal xenografts of human epithelial ovarian cancer in nude mice. Cancer Res. 1987; 47(10):2662–7. [PubMed: 3567897]
52. Jorfi S, et al. Inhibition of microvesiculation sensitizes prostate cancer cells to chemotherapy and reduces docetaxel dose required to limit tumor growth in vivo. Sci Rep. 2015; 5:13006. [PubMed: 26302712]
53. Drey EA, et al. Improving the accuracy of fetal foot length to confirm gestational duration. Obstet Gynecol. 2005; 105(4):773–8. [PubMed: 15802404]
54. Cunha G, et al. Methods for studying human organogenesis. Differentiation. 2016; 91(4–5):10–4. [PubMed: 26585195]
55. van Weerden WM, et al. Adrenal glands of mouse and rat do not synthesize androgens. Life Sci. 1992; 50(12):857–61. [PubMed: 1312193]
56. Cunha GR, Vanderslice KD. Identification in histological sections of species origin of cells from mouse, rat and human. Stain Technol. 1984; 59(1):7–12. [PubMed: 6206625]
57. Southgate J, Harnden P, Trejdosiewicz LK. Cytokeratin expression patterns in normal and malignant urothelium: a review of the biological and diagnostic implications. Histol Histopathol. 1999; 14(2):657–64. [PubMed: 10212826]
58. Moll R, Divo M, Langbein L. The human keratins: biology and pathology. Histochem Cell Biol. 2008; 129(6):705–33. [PubMed: 18461349]
59. Wu XR, et al. Uroplakins in urothelial biology, function, and disease. Kidney Int. 2009; 75(11): 1153–65. [PubMed: 19340092]
60. Scholzen T, Gerdes J. The Ki-67 protein: from the known and the unknown. J Cell Physiol. 2000; 182(3):311–22. [PubMed: 10653597]
61. Hiort O. The differential role of androgens in early human sex development. BMC Med. 2013; 11:152. [PubMed: 23800242]

62. Overland M, et al. Canalization of the Vestibular Plate in the Absence of Urethral Fusion Characterizes Development of the Human Clitoris: The Single Zipper Hypothesis. J Urol. 2016; 195(4 Pt 2):1275–83. [PubMed: 26926534]

63. Li Y, et al. Canalization of the urethral plate precedes fusion of the urethral folds during male penile urethral development: the double zipper hypothesis. J Urol. 2015; 193(4):1353–59. [PubMed: 25286011]

64. Shen J, et al. Complex epithelial remodeling underlie the fusion event in early fetal development of the human penile urethra. Differentiation. 2016; 92(4):169–182. [PubMed: 27397682]

65. Zheng Z, Armfield BA, Cohn MJ. Timing of androgen receptor disruption and estrogen exposure underlies a spectrum of congenital penile anomalies. Proc Natl Acad Sci U S A. 2015; 112(52):E7194–203. [PubMed: 26598695]

66. Madsen PO. Familial Female Pseudohermaphroditism with Hypertension and Penile Urethra. J Urol. 1963; 90:466–9. [PubMed: 14063383]

67. Ainger LE, et al. Female pseudohermaphroditism with penile urethra; report of an unusual case of congenital adrenal hyperplasia. AMA J Dis Child. 1958; 95(4):410–2. [PubMed: 13507876]

68. Wisniewski AB, et al. Complete androgen insensitivity syndrome: long-term medical, surgical, and psychosexual outcome. J Clin Endocrinol Metab. 2000; 85(8):2664–9. [PubMed: 10946863]

Abbreviations Used

AR	Androgen Receptor
BPA	Bisphenol A
DES	Diethylstilbestrol
DHT	Dihydrotestosterone
H&E	Hematoxylin and Eosin
IACUC	Institutional Animal Care and Use Committee
K6	Cytokeratin 6
K7	Cytokeratin 7
K10	Cytokeratin 10
PBS	Phosphate-Buffered Saline
PCR	Polymerase Chain Reaction
SCID	Severe Combined Immunodeficiency
SRY	Sex-Determining Region Y
UCSF	University of California, San Francisco

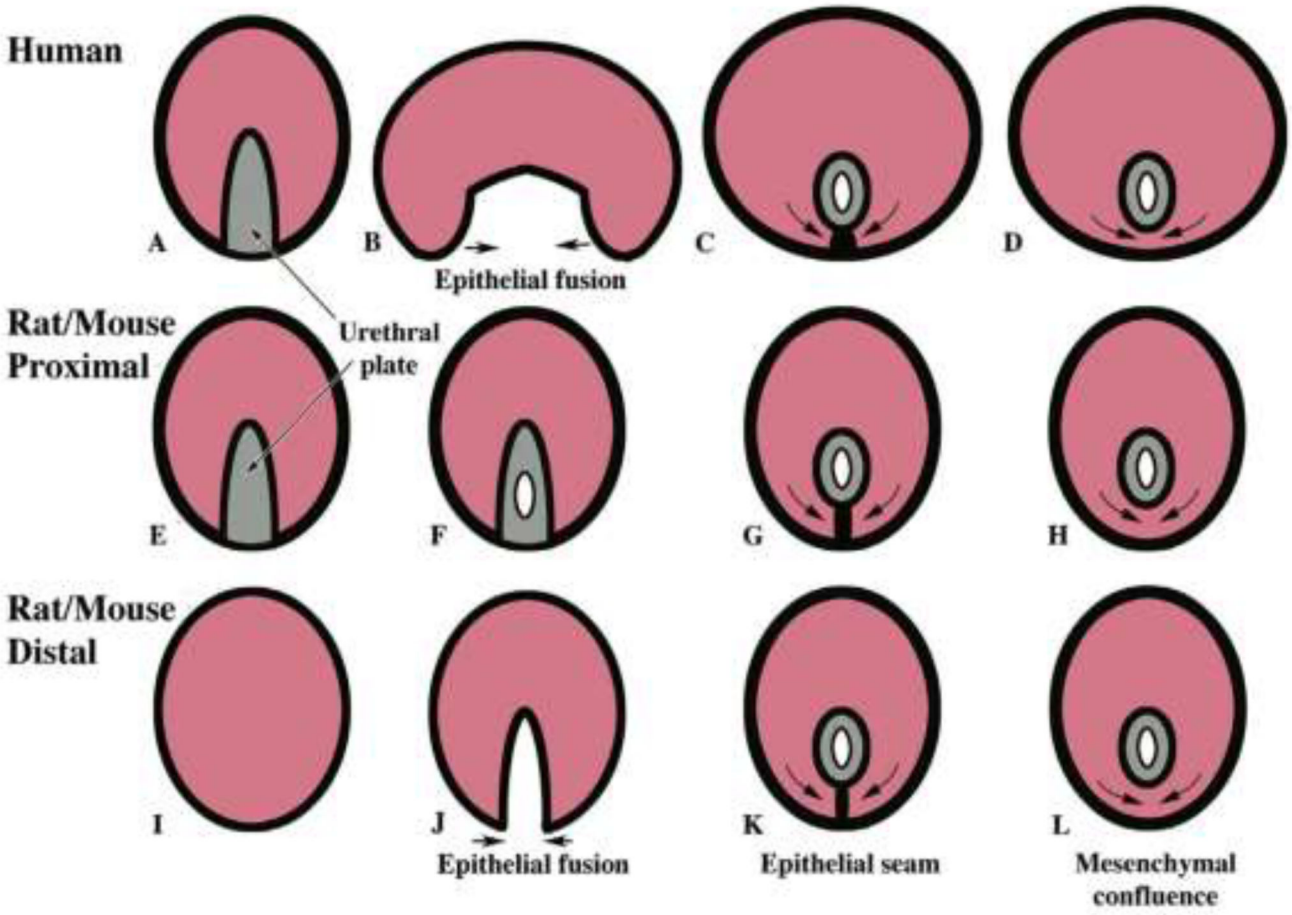

Figure 1.

Diagrammatic representations of urethral development in the human penile shaft (A–D), the human glans/rat and mouse proximal penis (E–H) and rat and mouse distal penis (I–L) showing similarities and differences. Note that the urethra in the shaft of the human penis forms by fusion of the urethral folds whereas this mechanism occurs only in the distal glans of the rat penis and mouse penis. In contrast, the urethra in the human glans forms by direct canalization of the urethral plate.

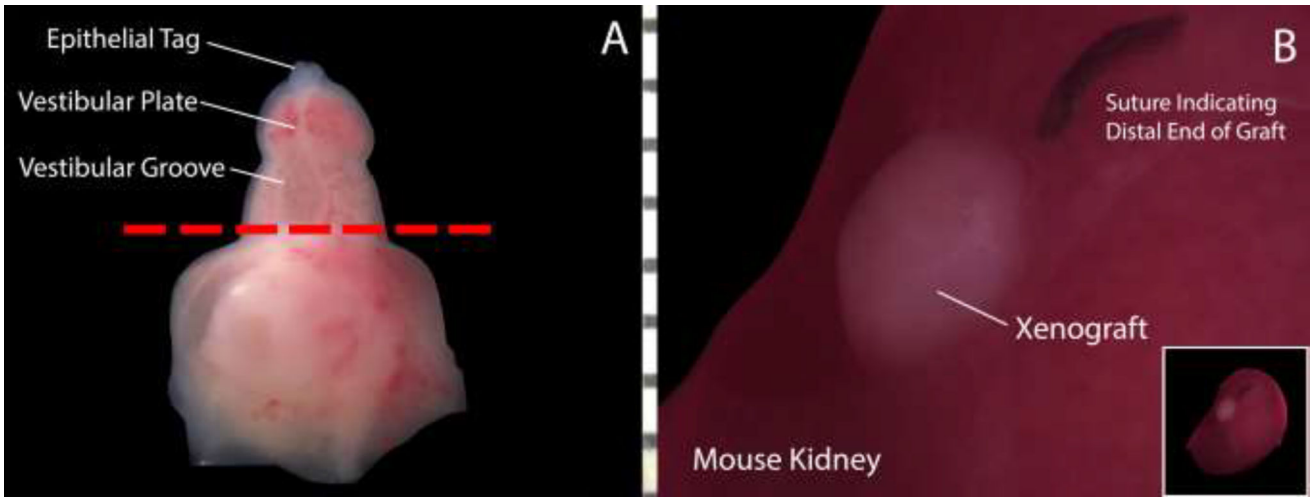

Figure 2.

Schematic demonstrating the xenografting process in a 10-week fetal clitoris. A: The distal genital tubercle is transected at the most proximal aspect of the open vestibular groove (red line) to ensure the absence of preexisting tubular structures and then grafted under the kidney capsule of an athymic mouse. B: Xenograft under mouse kidney capsule immediately prior to graft harvest. The nylon suture indicates the distal end/glans clitoris.

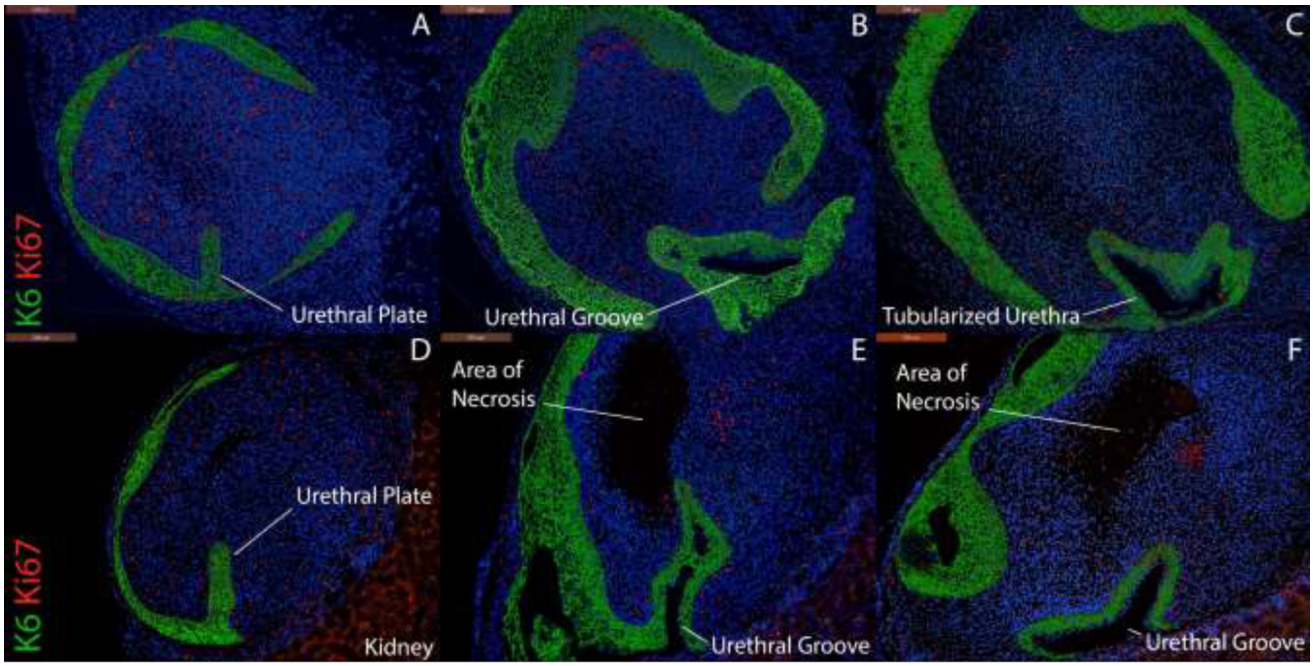

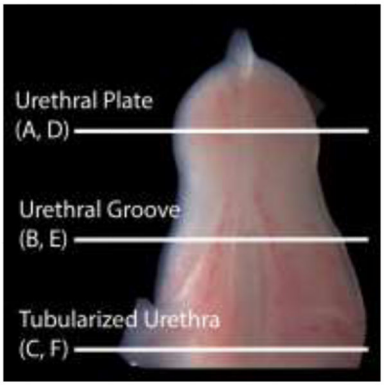

Gross 9.5-week human fetal penile specimen showing approximate levels of post-grafting histologic sections.

Figure 3.

Expression of Cytokeratin 6 (K6) and Ki-67 in two penile xenografts (Top: 8 weeks, Bottom: 9 weeks) grown for 14 days with DHT. Top, A–C, approximate section levels: Distal (A), mid-shaft (B) and proximal (C) transverse sections of a graft exhibiting a well-preserved urethral plate (A), urethral groove (B) and tubularized urethra (C). Ki-67 is expressed throughout the body of the penis, the urethral plate, the urethral groove and the tubularzied urethra. Bottom, D–F, approximate section levels: Distal (D), mid-shaft (E) and proximal (F) transverse sections of a second graft demonstrating central necrosis abutting but not enveloping developing urethral structures. Note the absence of Ki-67 in the area of necrosis and the presence of Ki-67 around the urethral groove.

Gross 9.5-week human fetal penile specimen showing approximate levels of post-grafting histologic sections.

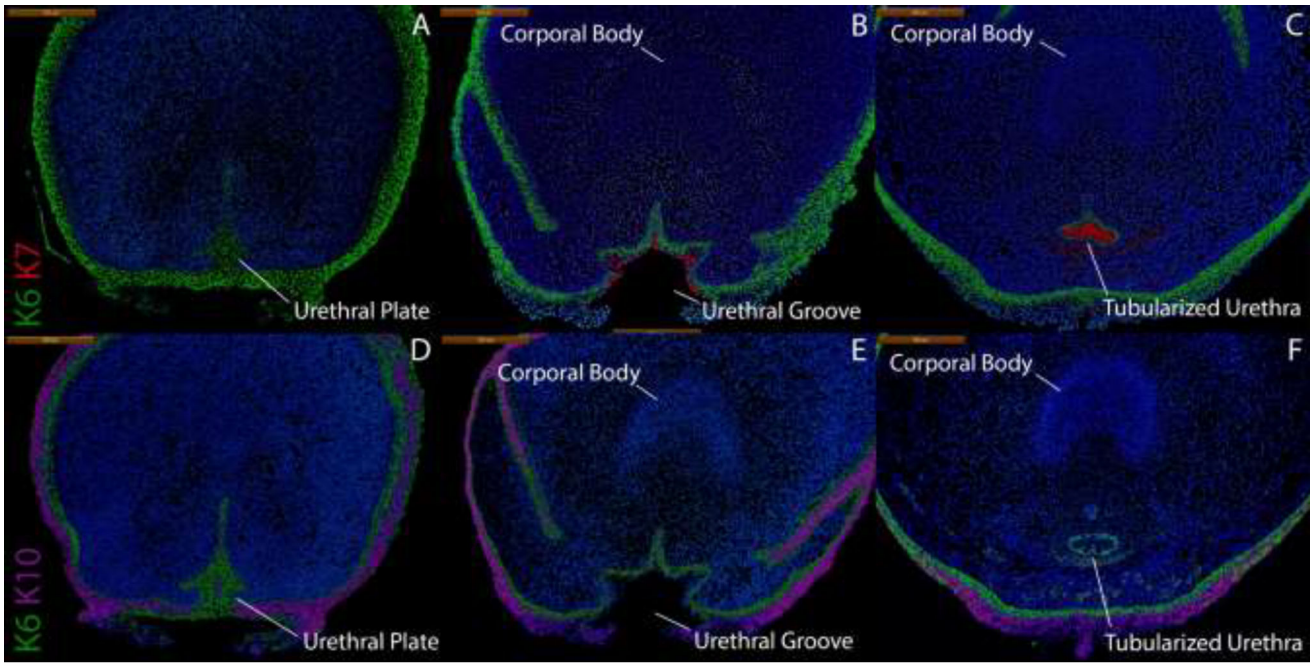

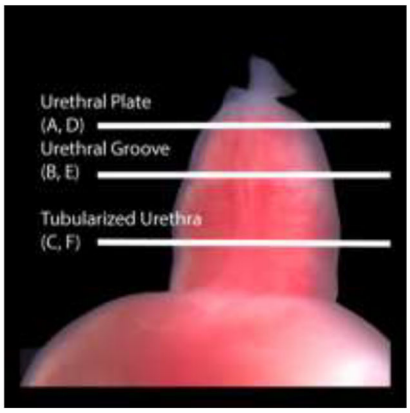

Gross 11-week human fetal penile specimen showing approximate levels of histologic sections.

Figure 4.

Cytokeratin staining of serial sections through a non-grafted 11-week human fetal penis. Top, A–C, approximate section levels: Distal (A), mid-shaft (B) and proximal (C) transverse sections stained for K6 and K7. K6 is expressed in the urethral plate and in basal cells of the surface epidermis, urethral groove and tubularized urethra. K7 is present only in apical layers of the urethral groove and the tubularized urethra. Uroplakin (Fig. 5) is expressed in the same areas as K7. Bottom, D–F, approximate section levels: Distal (D), mid-shaft (E) and proximal (F) sections through the same penis stained for K6 and K10. K6 is expressed as above. K10 is present in surface epidermis but absent in urethral structures.

Gross 11-week human fetal penile specimen showing approximate levels of histologic sections.

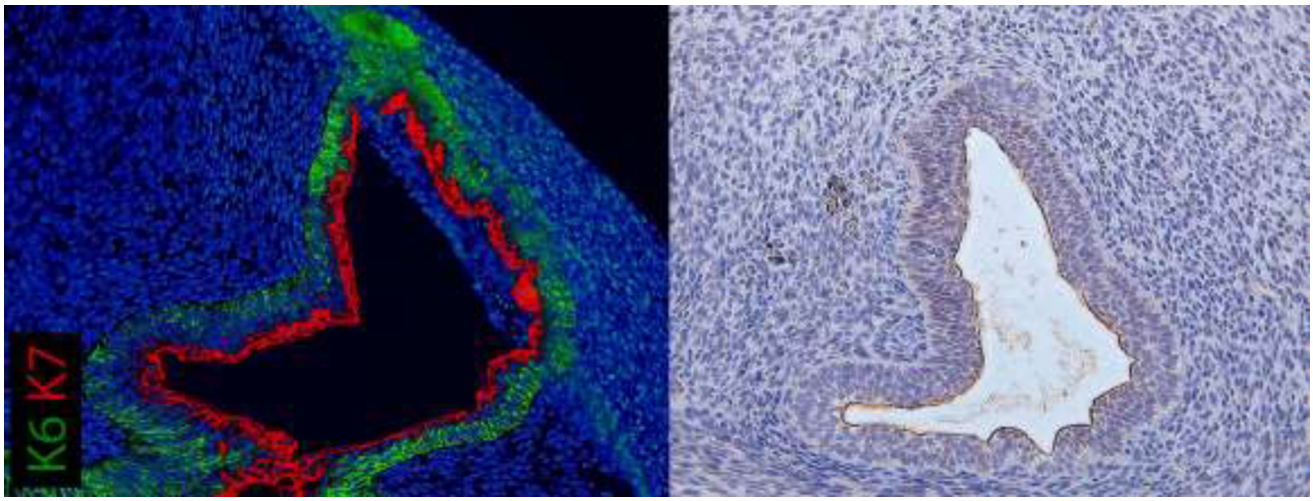

Figure 5.
Co-localization of uroplakin and K7 staining at apical surfaces of urethral epithelia of a xenograft exposed to DHT for 14 days. This xenograft formed a tubular urethra after two weeks of renal subcapsular grafting.

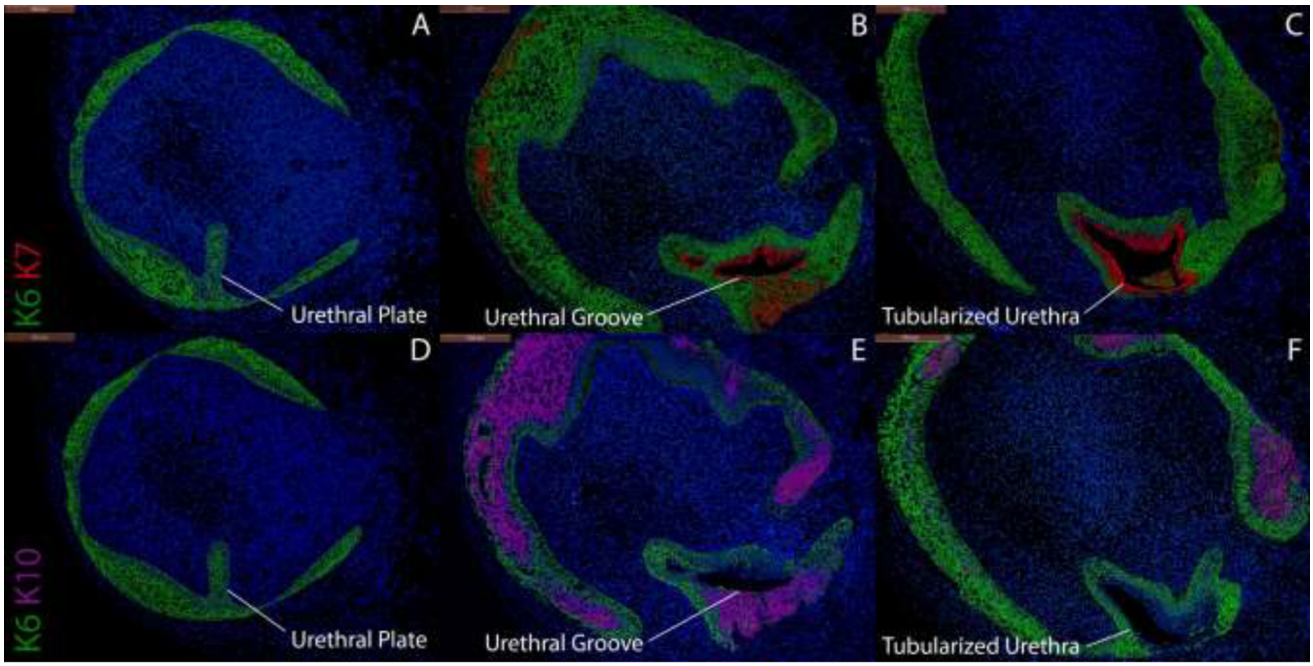

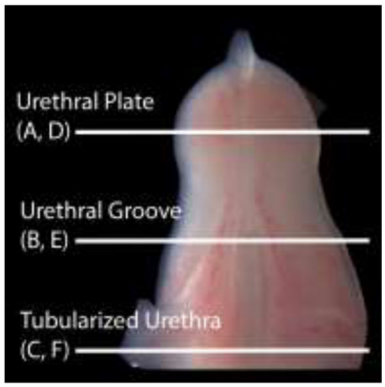

Gross 9.5-week human fetal penile specimen showing approximate levels of post-grafting histologic sections.

Figure 6.

Cytokeratin staining of serial sections through an 8-week human fetal penis grown for 14 days in a DHT-treated host. Top, A–C, approximate section levels: Distal (A), mid-shaft (B) and proximal (C) transverse sections stained for K6 and K7. K6 is expressed in the urethral plate (A), in basal cells of the surface epidermis, the urethral groove (B) and proximal tubularized urethra (C) of the graft. K7 is present in apical layers of the urethral groove (B) and the tubularized urethra (C) as in non-grafted penile specimens (Fig. 4). Bottom, D–F, approximate section levels: Distal (D), mid-shaft (E) and proximal (F) sections through the same xenograft stained for K6 and K10. K6 is expressed as above. K10 is present in apical layers of the surface epidermis but is absent in urethral structures, indicating that these are true urethral structures and not invaginations of surface epithelium.

Gross 9.5-week human fetal penile specimen showing approximate levels of post-grafting histologic sections.

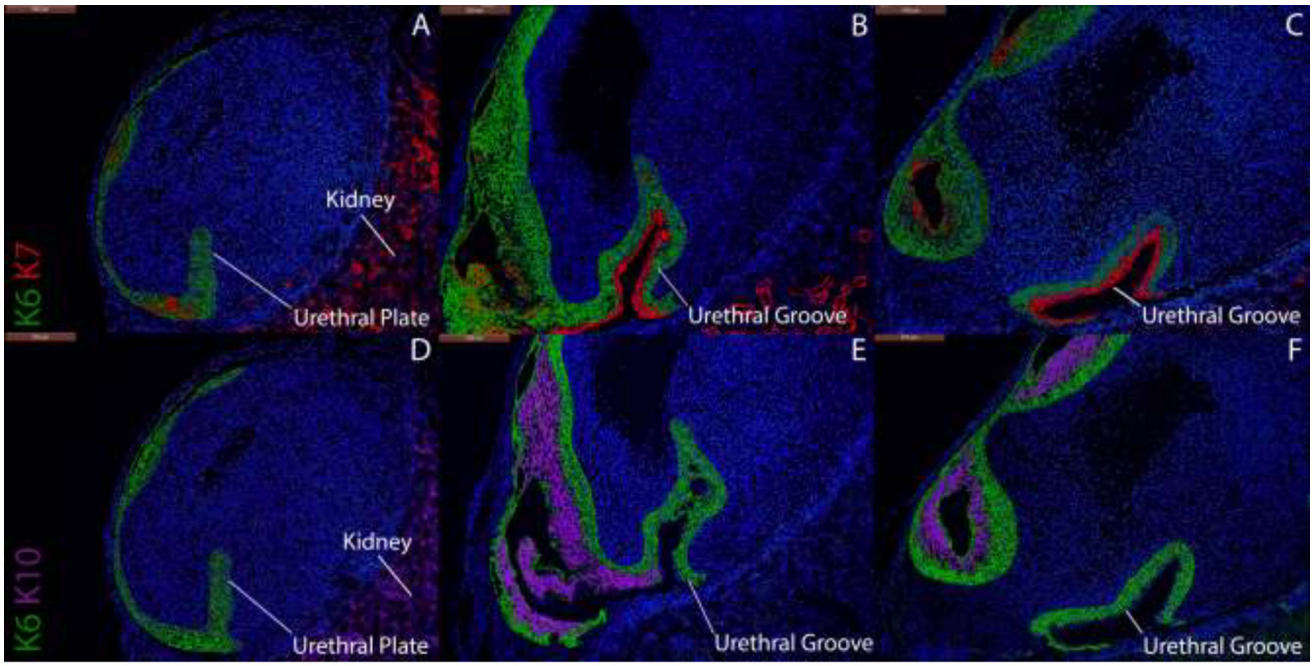

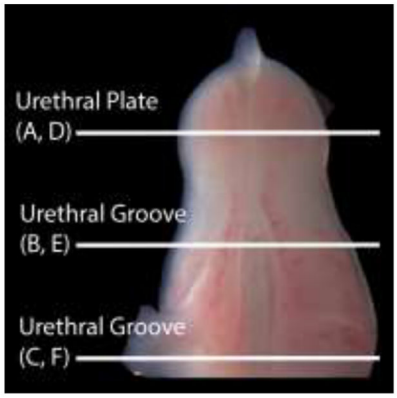

Gross 9.5-week human fetal penile specimen showing approximate levels of post-grafting histologic sections.

Figure 7.

Cytokeratin staining of serial sections through a 9-week human fetal penis grown for 14 days without hormones. Top, A–C, approximate section levels: Distal (A), mid-shaft (B) and proximal (C) transverse sections stained for K6 and K7. K6 is expressed in the urethral plate and basal cells of the surface epidermis and in basal layers of the urethral groove. K7 is present only in apical layers of the dorsal aspect of the urethral groove) as in non-grafted penile and clitoral specimens (Figs. 4, 8). Bottom, D–F, approximate section levels: Distal (D), mid-shaft (E) and proximal (F) sections through the same xenograft stained with K6 and K10. K6 is expressed as above. K10 is present in apical cells of the surface epidermis,

the lateral and ventral aspects of the urethral groove and is absent in the dorsal aspect of the urethral groove as is seen in non-grafted penile and clitoral specimens.
Gross 9.5-week human fetal penile specimen showing approximate levels of post-grafting histologic sections.

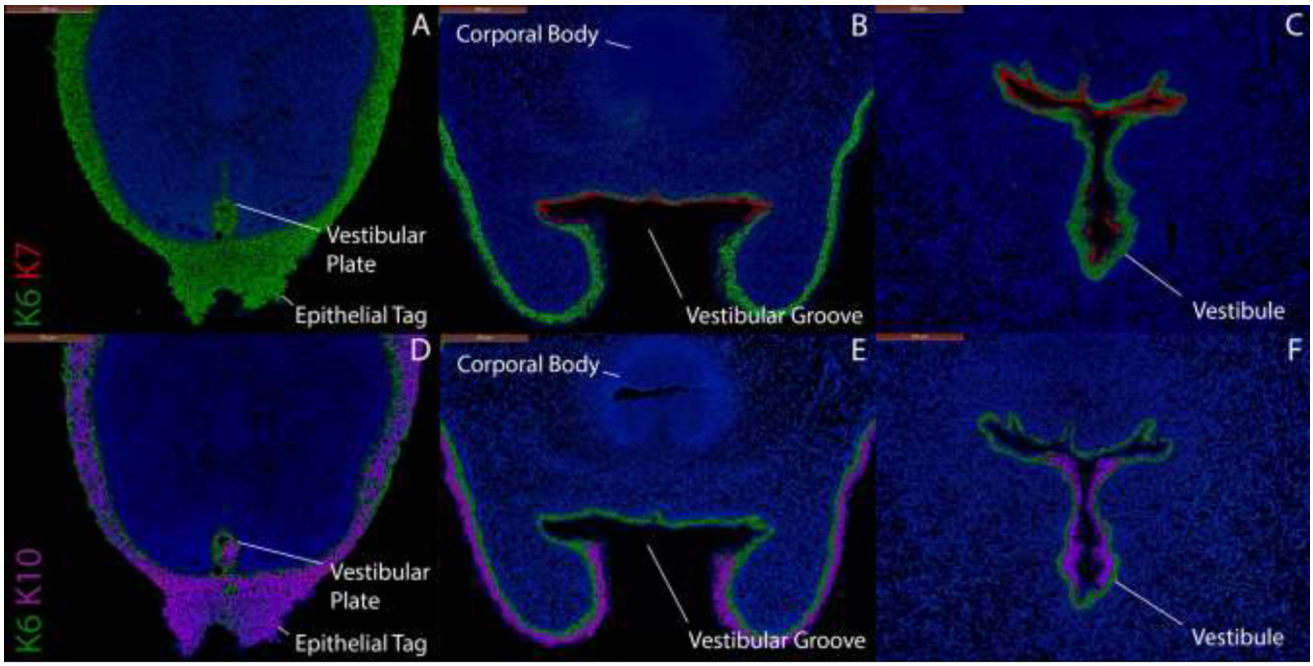

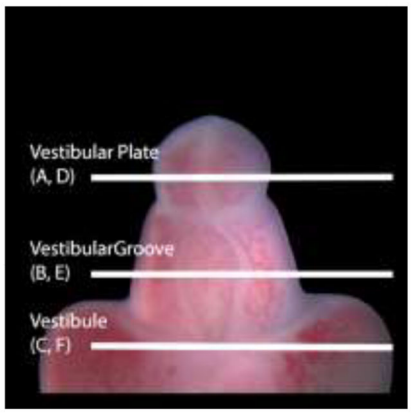

Gross 11-week human fetal clitoral specimen showing approximate levels of histologic sections.

Figure 8.

Cytokeratin staining of serial sections through a non-grafted 11-week fetal clitoris. Top, A–C, approximate section levels: Distal (A), mid-shaft (B) and proximal (C) transverse sections stained for K6 and K7. K6 is expressed in the vestibular plate and in basal layers of surface epidermis, the vestibular groove and vestibule. K7 is present only in apical layers of the dorsal vestibular groove and vestibule. Uroplakin (not shown) is expressed in the same areas as K7. Bottom, D–F, approximate section levels: Distal (D), mid-shaft (E) and proximal (F) sections through the same clitoris stained for K6 and K10. K6 is expressed as above. K10 is present in surface epithelial structures, ventral and lateral aspects of the vestibule but absent in the dorsal aspects of these structures.

Gross 11-week human fetal clitoral specimen showing approximate levels of histologic sections.

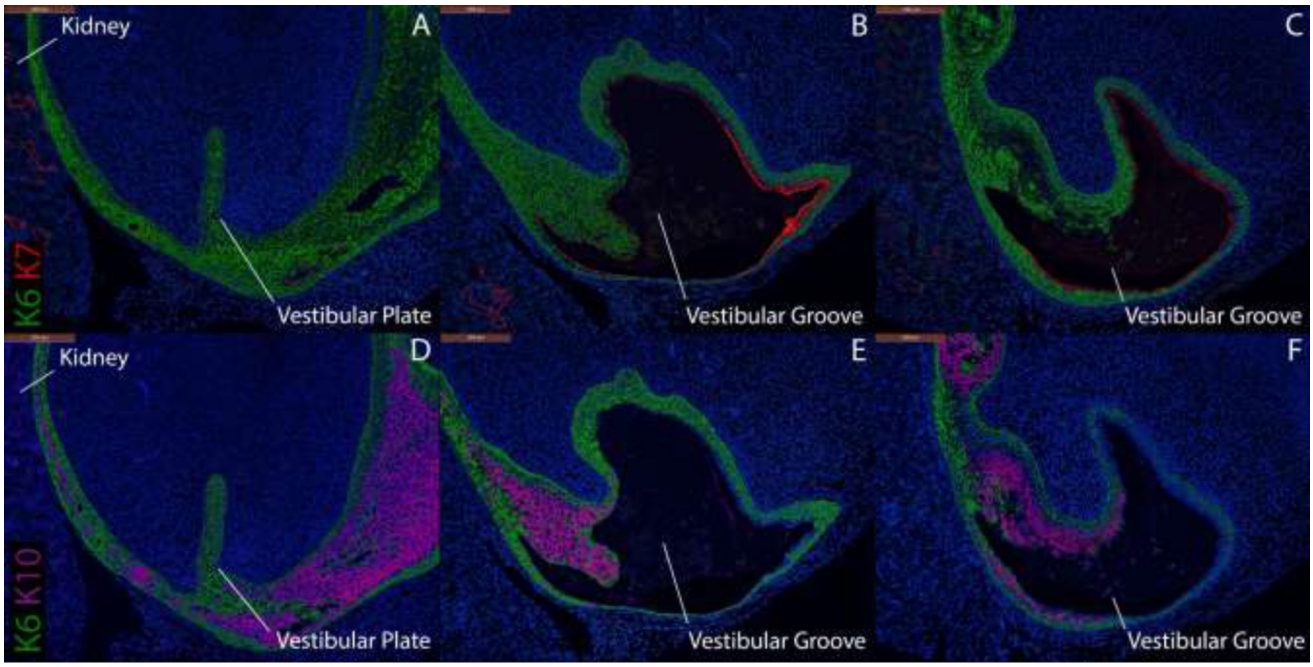

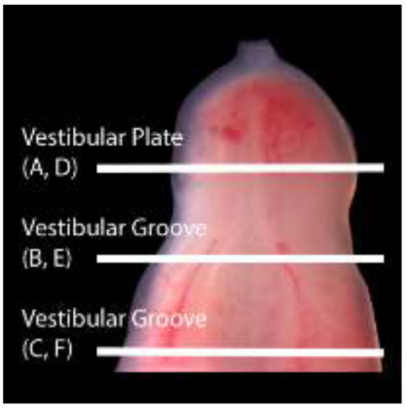

Gross 10-week human fetal clitoral specimen showing approximate levels of post-grafting histologic sections.

Figure 9.

Cytokeratin staining of serial sections through a 9.5-week human fetal clitoris grown for 14 days in an untreated castrated host. Top, A–C, approximate section levels: Distal (A), mid-shaft (B) and proximal (C) transverse sections stained for K6 and K7. K6 is expressed in the vestibular plate, in basal cells of the surface epidermis and in basal layers of the vestibular groove of the graft. K7 is present only in apical layers of the dorsal aspect of the vestibular groove as in non-grafted clitoral specimens (Fig. 8). Bottom, D–F, approximate section levels: Distal (D), mid-shaft (E) and proximal (F) sections through the same xenograft stained with K6 and K10. K6 is expressed as above. K10 is present in apical cells of the

surface epidermis, the lateral and ventral aspects of the vestibular groove and is absent in the dorsal aspect of the vestibular groove as is seen in non-grafted clitoral specimens.
Gross 10-week human fetal clitoral specimen showing approximate levels of post-grafting histologic sections.

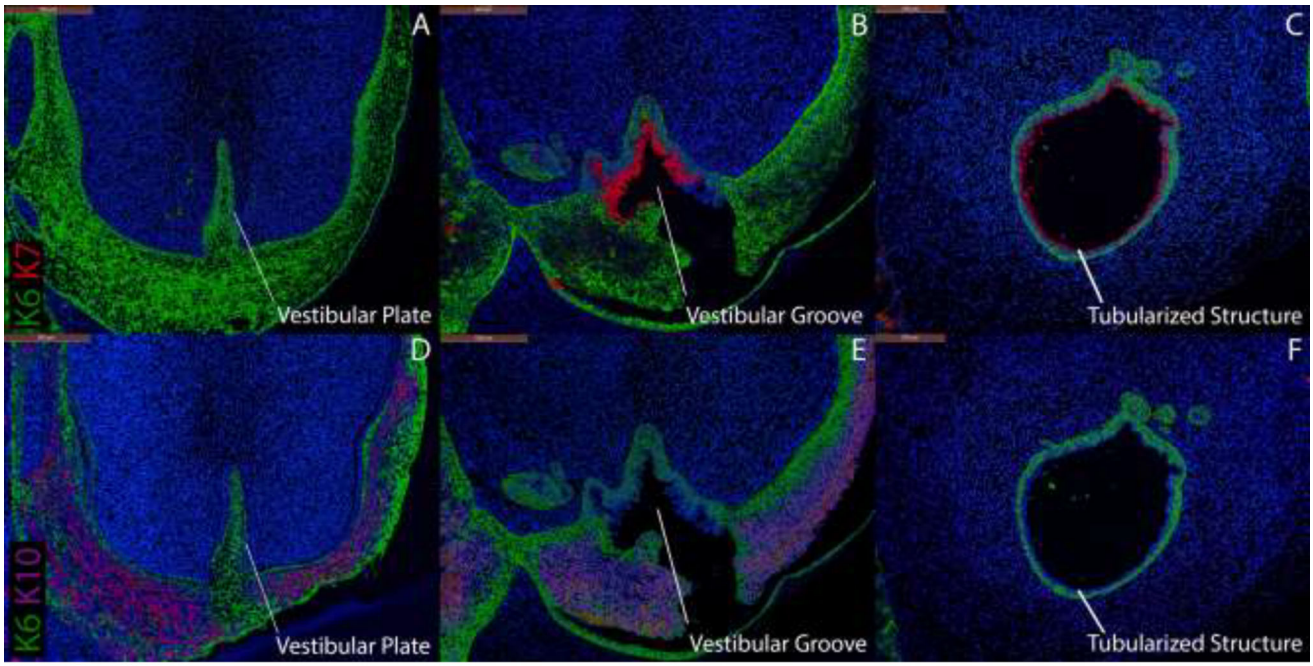

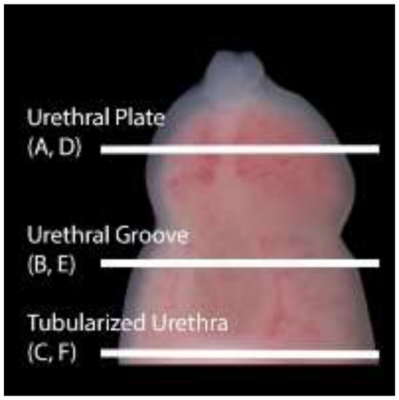

Gross 10-week human fetal clitoral specimen showing approximate levels of post-grafting histologic sections.

Figure 10.

Cytokeratin staining of serial sections through a 9.5-week human fetal clitoris grown for 14 days with DHT. Top, A–C, approximate section levels: Distal (A), mid-shaft (B) and proximal (C) transverse sections stained for K6 and K7. K6 is expressed in the vestibular plate, in basal cells of the surface epidermis, the vestibular groove and the proximal tubularized urethral structure that formed within the graft. K7 and uroplakin (not shown) are present in apical layers of the vestibular groove and the tubularized urethral structure as in non-grafted penile specimens (Fig. 4). Bottom, D–F, approximate section levels: Distal (D), mid-shaft (E) and proximal (F) sections through the same xenograft stained for K6 and K10.

K6 is expressed as above. K10 is present in apical layers of the surface epidermis (D–E) but is absent in the tubularized urethral structure.

Gross 10-week human fetal clitoral specimen showing approximate levels of post-grafting histologic sections.

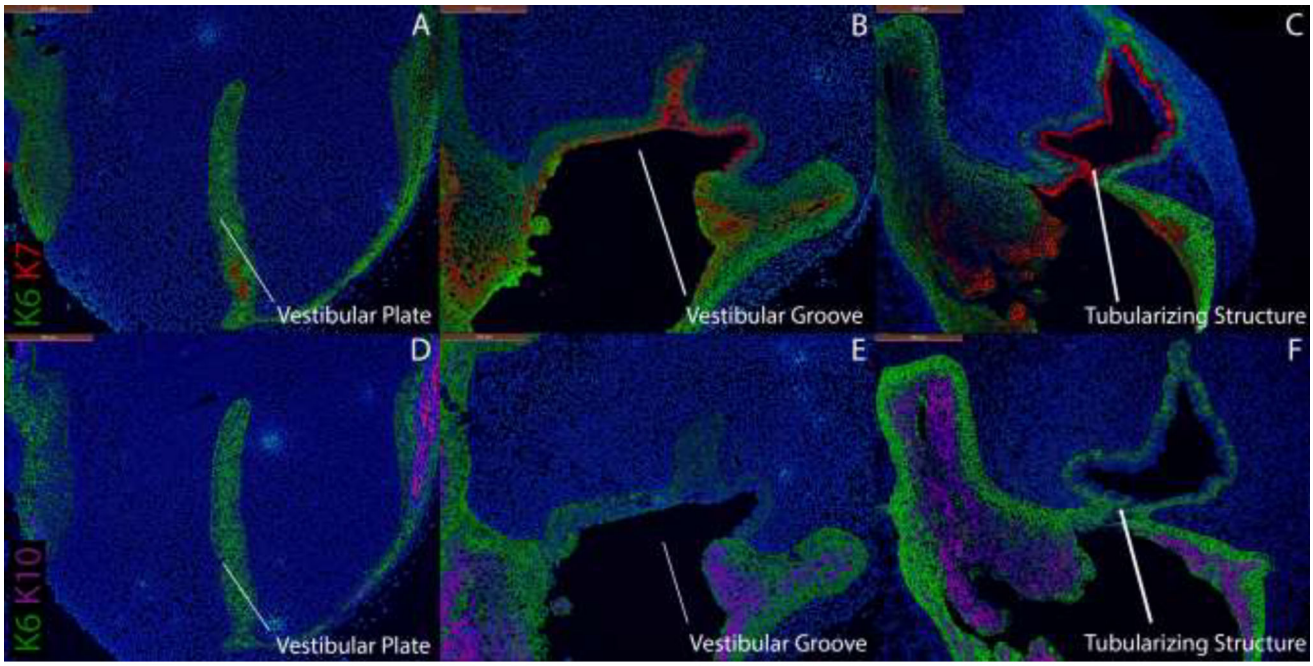

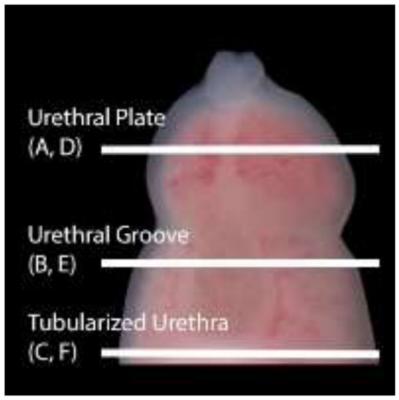

Gross 10-week human fetal clitoral specimen showing approximate levels of post-grafting histologic sections.

Figure 11.

Cytokeratin staining of serial sections through an 8.5-week human fetal clitoris grown for 14 days with DHT. Top, A–C, approximate section levels: Distal (A), mid-shaft (B) and proximal (C) transverse sections stained for K6 and K7. K6 is expressed in the vestibular plate, in basal cells of the surface epidermis, the vestibular groove and the actively tubularizing urethral structure of the graft. K7 and uroplakin (not shown) are present in apical layers of the vestibular groove and the tubularizing urethral structure as in non-grafted penile specimens (Fig. 4). Bottom, D–F, approximate section levels: Distal (D), mid-shaft (E) and proximal (F) sections through the same xenograft stained for K6 and K10. K6 is

expressed as above. K10 is present in apical layers of the surface epidermis (D–E) but is absent in urethral/vestibular structures.

Gross 10-week human fetal clitoral specimen showing approximate levels of post-grafting histologic sections.

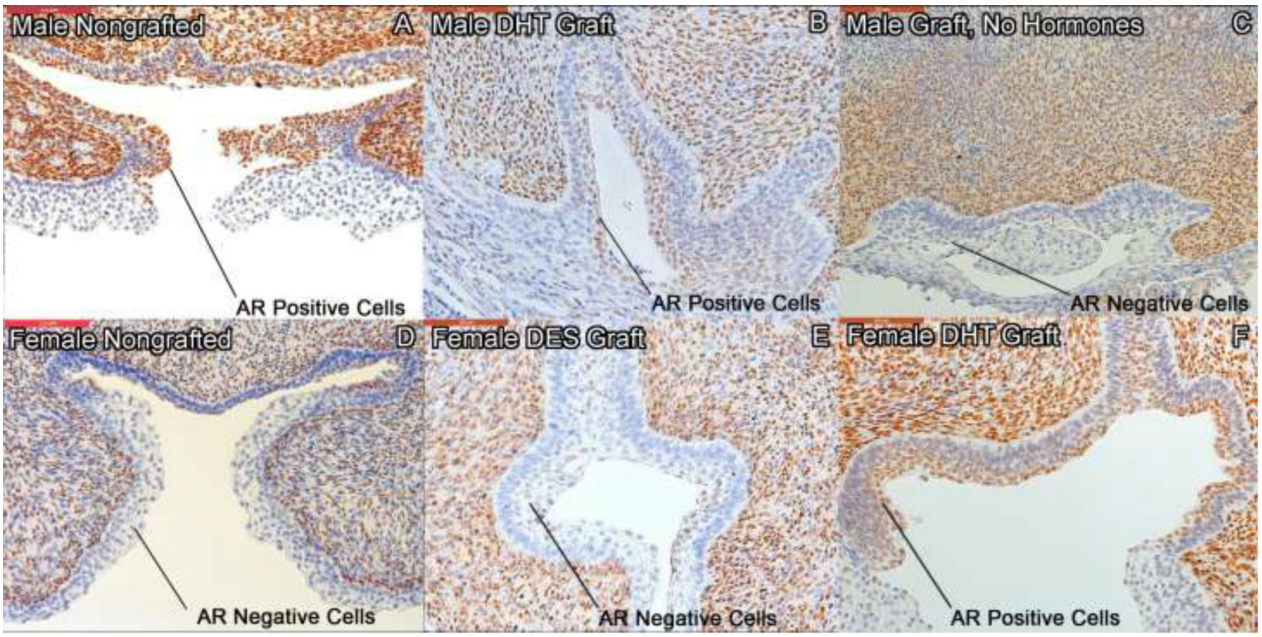

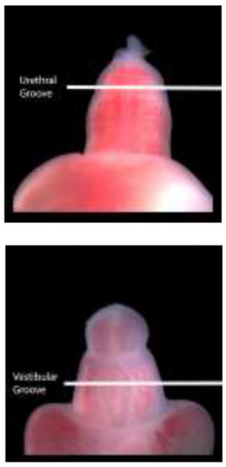

Gross 11-week human fetal penile (top) and clitoral (bottom) specimens showing approximate levels of histologic sections.

Figure 12.

Androgen receptor (AR) staining of non-grafted human specimens and human genital xenografts. Top, A–C, penile specimens sectioned at the level of the urethral groove: AR staining of an 11-week human fetal non-grafted penis (A), a 9-week penis grown for 14 days with DHT (B), and an 8-week penis grown for 14 days without hormones (C). AR is expressed in the epithelium of the dorsal urethral groove and in the urethral folds of normal penile specimens and penile grafts grown with DHT (A, B) but absent in penile specimens grown without hormone (C). Bottom, D–F, clitoral specimens sectioned at the level of the vestibular groove: AR staining of an 11-week human fetal non-grafted clitoris (D), a 9.5

week clitoris grown for 14 days with DES (E) and an 8.5 week clitoris grown for 14 days with DHT (F). AR stains negative in the lateral aspects of the vestibular groove of normal clitoral specimens and clitoral grafts grown with DES (D, E), but stains positive in clitoral grafts grown with DHT (F).

Gross 11-week human fetal penile (top) and clitoral (bottom) specimens showing approximate levels of histologic sections.

Table 1

Primary and secondary antibodies used in control external genital and xenograft staining by manufacturer and dilution strength

Antigen	Primary Antibody (Manufacturer)	Dilution	Secondary Antibody (Manufacturer)	Dilution
Cytokeratin 6 (K6)	Acris Antibodies, Rockville MD, USA	1:200	AlexaFluor® 488 goat anti-rabbit, Thermo Fisher Scientific, Waltham MA, USA	1:500
Cytokeratin 7 (K7)	E. Birgitte Lane, PhD Laboratory, Dundee, UK	1:5	AlexaFluor® 555 goat anti-mouse, Thermo Fisher Scientific, Waltham MA, USA	1:500
Cytokeratin 10 (K10)	Agilent, Santa Clara, CA, USA	1:50	AlexaFluor® 555 goat anti-mouse Thermo Fisher Scientific, Waltham MA, USA	1:500
Uroplakin (UPK)	Nichriei Biosciences, Tokyo, Japan	1:1000	GE Healthcare, Chicago, Il, USA	1:100
Ki-67	Leica Biosystems, Wetzlar, Germany	1:100	AlexaFluor® 555 goat anti-mouse, Thermo Fisher Scientific, Waltham MA, USA	1:500
Androgen Receptor (AR)	GeneTex, Irvine, CA, USA	1:100	GE Healthcare, Chicago, Il, USA	1:100